

Trapping reactions of reactive carbonyl species with tea polyphenols in simulated physiological conditions

Chih-Yu Lo¹, Shiming Li¹, Di Tan¹, Min-Hsiung Pan², Shengmin Sang³ and Chi-Tang Ho¹

¹Department of Food Science, Rutgers University, New Brunswick, NJ, USA

²Department of Seafood Science, National Kaohsiung Marine University, Kaohsiung, Taiwan

³Department of Chemical Biology, Susan Lehman Cullman Laboratory for Cancer Research, Ernest Mario School of Pharmacy, Rutgers University, Piscataway, NJ, USA

The carbonyl stress that leads to the formation of advanced glycation end products (AGEs) in diabetes mellitus has drawn much attention recently. Reactive alpha-dicarbonyl compounds, such as glyoxal (GO) and methylglyoxal (MGO), have been shown to be a high potential glycation agent *in vitro* and *in vivo*. In this study, epicatechins in green tea and theaflavins in black tea were found to be able to reduce the concentration of MGO in physiological phosphate buffer conditions. Modified MGO derivatization for GC/flame ionization detector (FID) method in quantification was systematically conducted. In molar ratio of 3 (MGO/polyphenol), theaflavin-3,3'-digallate (TF3) in theaflavins and (–)-epigallocatechin (EGC) in epicatechins showed the highest MGO reduction at 66.65 and 45.74%, respectively, after 1 h of incubation. In kinetic study (molar ratio of MGO/polyphenol = 1:1), rapid MGO reduction occurred within 10 min. Identities of primary adducts between (–)-epigallocatechin gallate (EGCG) and MGO were determined. Newly generated stereoisomers at the C8 position of EGCG A-ring were isolated with a chiral column, and structurally confirmed by 2-D NMR analyses.

Keywords: Carbonyl stress / Maillard reaction / Methylglyoxal / Reactive carbonyl species / Tea polyphenols

Received: July 4, 2006; revised: September 19, 2006; accepted: September 19, 2006

1 Introduction

Associated with hyperglycemia in both Types I or II diabetic subjects, elevated levels of glucose in the body fluid enhance imbalanced physiological metabolisms. Overproduction of reactive oxygen species (ROS), such as superoxide radical ($O_2^{\cdot-}$), hydrogen peroxide (H_2O_2), and the hydroxyl radical (OH \cdot), play an important role in cell injury, aging, and clinical disorders [1, 2]. However, increasing evidence in both clinical and experimental studies discuss the roles of various reactive carbonyl species (RCS) [3–5].

Many microvascular and macrovascular implications such as nephropathy, retinopathy, peripheral neuropathy, and arteriosclerosis are the chronic accumulation of advanced glycation end products (AGEs) in diabetes mellitus [6–9]. AGEs are the products of the Maillard reaction in biological systems. High glucose concentration in physiological systems leads to the formation of RCS. Further reaction will lead to the generation of stable AGEs adducts. Among AGEs, the three most important glycation biomarker categories used in quantitative screening of AGE accumulation in animal study were hydroimidazolones, monolysyl adducts (*N* ϵ -carboxymethyl-lysine and *N* ϵ -1-carboxyethyl-lysine), and *bis*(lysyl)imidazolium crosslinks and pentosidine [3].

The complexities of AGE generation arise from multiple branches in the reaction complex. Among various RCS, the most noted α -oxoaldehydes are 3-deoxyglucosone (3-DG), glyoxal (GO), and methylglyoxal (MGO). In food chemistry, they are important precursors of aroma and color generations. Consequently, these reactive compounds in processed food affect shelf lives, nutrition values, and health concerns [10–12]. In biochemistry, MGO is identified as

Correspondence: Professor Chi-Tang Ho, Department of Food Science, Rutgers University, 65 Dudley Road, New Brunswick, NJ 08901–8520, USA

E-mail: ho@aesop.rutgers.edu

Fax: +1-732-932-6776

Abbreviations: AGEs, advanced glycation end products; EC, (–)-epicatechin; ECG, (–)-epicatechin-3-gallate; EGC, (–)-epigallocatechin; FID, flame ionization detector; GO, glyoxal; HMBC, heteronuclear multiple quantum multiple bond correlation; HSQC, heteronuclear single-quantum correlation; IS, internal standard; PY, pyrogallol; TF1, theaflavin; TF2, theaflavin-monogallate; TF3, theaflavin-3,3'-digallate

one of the most important precursors of AGEs *in vivo* and is generated from the metabolism of ketone bodies, degradation of threonine, and by the fragmentation of triosephosphates [13–15]. Many factors that manipulate 3-DG, GO, and MGO concentrations *in vitro* were investigated [16]. Recently, MGO bindings proteins were reported as well as the identification of DNA adducts of MGO [17]. Although α -oxoaldehydes, GO and MGO, are subjected to be transformed from dicarbonyl compounds into their corresponding α -hydroxyacids through glyoxalase system, a glutathione (GSH) dependent enzymatic system, GSH depletion in oxidative stress is an endogenously physiological phenomenon [18]. Therefore, studies on the prevention of RCS accumulation in body fluid will be strategies in reducing the occurrence of diabetic complications.

Many organic chemical synthetic compounds were demonstrated to have high values in AGE inhibitions [19]. In consideration of antioxidative property of polyphenols, certain flavonoids had shown more effective inhibition of AGEs formation than aminoguanidine, a well-known AGEs inhibitor [20]. More recently, researchers had documented the effects of added natural phenolic compounds on the generation of reactive carbonyl intermediates from Maillard reaction [21]. In the present study, the importance of natural antioxidants in MGO level reduction under physiological conditions is illustrated.

2 Materials and methods

2.1 Materials

The dicarbonyl molecule used in this study was MGO. MGO, 40 wt% in water, PBS (pH 7.4), phosphate–citrate buffer tablet, *O*-(2,3,4,5,6-pentafluorobenzyl)-hydroxylamine hydrochloride (PFBHA), gallic acid (GA), pyrogallol (PY), (–)-epicatechin (EC), anhydrous pyridine, acetic anhydride, and Sephadex LH-20 gel were purchased from Sigma-Aldrich (St. Louis, MO, USA). 2-Chlorobenzaldehyde (internal standard; IS) and tannase from *Aspergillus ficuum* were purchased from Fluka (Milwaukee, WI, USA). Glass threaded vials (22.2 mL; 23 mm \times 85 mm; od \times H), absolute ethanol, hexanes, ethyl acetate, ACN, water (HPLC grade), and methylene chloride were purchased from Fisher Scientific (Fairlawn, NJ, USA). Ethanol (95%) was purchased from VWR Scientific (South Plainfield, NJ, USA). (–)-Epigallocatechin gallate (EGCG; 100% pure) was provided by Mitsui Norin (Shizuoka, Japan). TLC was performed on 250 μ m thickness, 2–25 μ m particle size TLC plates (Sigma-Aldrich). Theaflavins 28% crude extract was obtained from Hunan Kinglong Bio-resource (Hunan, China).

2.2 Preparation of (–)-epigallocatechin (EGC), (–)-epicatechin-3-gallate (ECG), theaflavin (TF1), theaflavin-monogallate (TF2), and theaflavin-3,3'-digallate (TF3)

In the reaction of EGCG hydrolysis reaction: 300 mg of EGCG was dissolved in 10 mL of 0.05 M, pH 5.0, phosphate–citrate buffer solution. Tannase (100 mg) was added to the solution and stirred continuously for 20 min. The reaction solution was dried under vacuum. After applying reaction mixtures onto a Sephadex LH-20 column which was eluted with 95% ethanol, pure EGC was collected for further study.

Ethyl acetate fraction of theaflavin extract was subjected to a Sephadex LH-20 column and eluted with acetone solution (40% v/v). According to their elution sequences, four fractions were collected. They are catechins, TF1, TF2, and TF3. ECG was obtained from catechins fraction, followed by the same procedure as EGC purification. The emphasis on TF2s composition was further pointed out here. TF2 was a mixture of theaflavin-3-monogallate (TF2) and theaflavin-3'-monogallate (TF2'). They cannot be isolated into pure compound under LH-20 chromatography. The composition ratio for TF2/TF2' was 3:1 after being quantified by the HPLC method [22].

2.3 Methods

2.3.1 Reaction of MGO with polyphenols

The dry powder form of PBS was packed in a foil pouch initially. After the dry powder dissolves in 1 L of deionized water, it yields 0.01 M PBS which contains 0.138 M NaCl; 0.0027 M KCl; pH 7.4, at 25°C. This condition has been specifically developed for use in immunoassay procedures and used in physiological studies. 2.00 mM MGO and 5.33 mM of each individual polyphenol compound, PFBHA and IS (2-chlorobenzaldehyde) in PBS were freshly prepared before the experiment. MGO (8 mL) was mixed with 1 mL of PBS or a polyphenol PBS solution. After capping the vials, the sample was stirred vigorously for 5 s. Control samples, MGO and PBS only, were placed in the salt/ice bath and other vials were placed in the 37°C water bath incubator and shaken at 40 rpm speed. After 1 h incubation, appropriate amounts of PFBHA and IS were added to the samples. Samples were stirred vigorously for another 5 s before derivatization.

For the derivatization reaction between MGO, IS and PFBHA, the shaking speed was increased to 50 rpm instead of 40 rpm but the temperature was kept the same at 37°C. After the reaction was completed, the *O*-PFB-oximes derivatives were extracted with 4 mL of methylene chloride three times. The organic phase was dried over anhydrous sodium

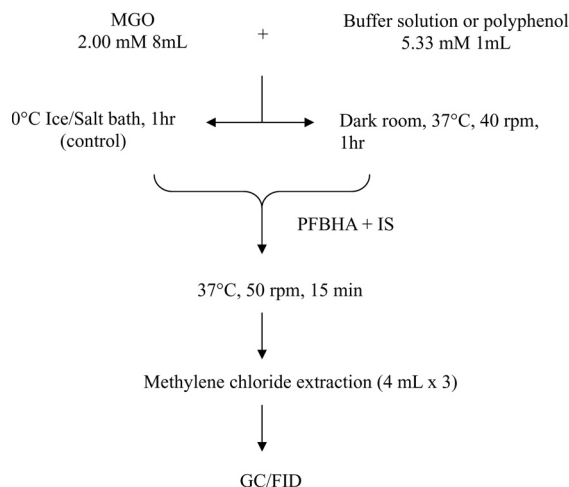


Figure 1. Sample composition, incubation conditions, and derivatization reaction procedure before GC analysis.

sulfate. The volume was reduced to around 0.5 mL under gentle nitrogen flow before GC/flame ionization detector (FID) analysis. The flow chart indicating the composition and treatment procedure before GC/FID analysis of sample is shown in Fig. 1. The entire procedure was repeated three times to get triplicate results for analyses. The amount of decreased oximes in triplicate samples was expressed as mean \pm SD.

2.3.2 Incubation-time course study

In order to learn more about the reaction between MGO and polyphenols in green and black tea, a kinetic experiment was set up. MGO (2.00 mM) and 5.33 mM EC, ECG, EGC, EGCG, TF1, TF2, and TF3 were freshly prepared in pH 7.4 PBS as in the previous section. In MGO study: 2.67 mL MGO was transferred and mixed with 1.00 mL of PBS (control) and individual epicatechin or theaflavin. The vial was capped and stirred vigorously for 5 s.

The incubation conditions were the same as in section 2.3.1. The time points were set at 5, 10, 20, 30, and 40 min. At each specific time point, samples were taken out from the incubator and put into salt/ice bath immediately before the subsequent derivatization. After all the samples were collected, the derivatization and extraction procedures were the same as in section 2.3.1 but only 2 mL methylene chloride (three times) was used in extraction. The extracted samples were concentrated by gentle nitrogen gas. The flow chart indicating the composition and treatment procedure before GC/FID analysis of sample is shown in Fig. 2. The amount of oximes in 0 h samples was treated as the initial amount. The decrease of dicarbonyl compounds was monitored as a function of time. Duplicate samples were obtained at each time point. Values were expressed as mean \pm 1/2 range.

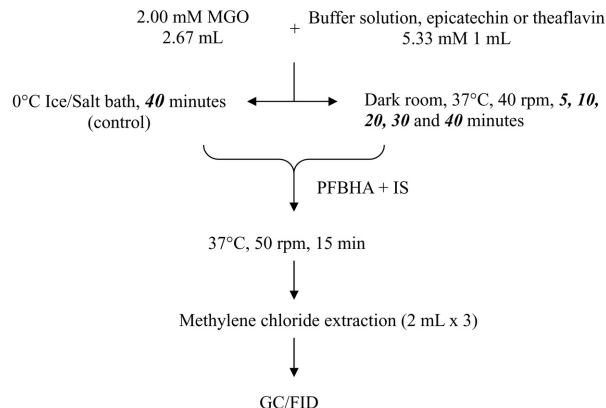


Figure 2. Sample composition, incubation time points, and derivatization reaction procedure for kinetic study of MGO and tea polyphenol.

2.3.3 GC method for relative MGO residue measurement

In the past few years, several studies have monitored the role of carbonyl stress, especially for those dicarbonyl compounds such as GO and MGO. Several methods had been evaluated. The goal was to find a simple and effective method with less required amount of sample treatment to achieve higher accuracy. The capillary GC method was chosen and performed as following:

The analyses of derivative volatiles were performed with an Agilent Gas Chromatograph (Agilent Technologies, Palo Alto, CA, USA). The Agilent Gas Chromatograph (6850 Series) was equipped with an Agilent autosampler (7683 Series Injector) and an FID. Samples (1 μ L) were analyzed on an HP-1 MS dimethylpolysiloxane silica capillary column (part number 19091S-733E, 30 m \times 0.25 mm id, film thickness 1.00 μ m (Agilent, Wilmington, DC, USA). The injector temperature was 250°C and detector temperature was 300°C with hydrogen, air, and makeup gas (helium) flow rate at 30.0, 300.0, and 5.0 mL/min, respectively. The injector was in 1:1 split mode. The 1.0 mL/min constant carrier gas (helium) flow rate was set. The GC oven temperature was programmed as follows: the initial oven temperature 40°C was held for 0 min and increased to 208°C at the rate of 4°C/min held for 0 min. Then the temperature was increased to 260°C final temperature at the rate of 40°C/min and held for 3 min. The total run time was 46.3 min.

2.3.4 Preparation of EGCG/MGO reaction products

The large amount of EGCG is used as a model reaction to investigate the reaction products of MGO and green tea polyphenols. Four vials which contained 4 mL of 0.11 M EGCG in PBS and 0.5 mL of 0.55 M MGO in PBS were

incubated at 37°C in a water bath for 20 min. The EGCG/MGO solutions were combined and dried under vacuum. The dry powder was dissolved in 95% ethanol before being applied to a Sephadex LH-20 column. The 95% ethanol had been used for the whole elution process. The fractions were collected by a fraction collector. The purity of each fraction was checked by TLC test. One pure adduct A rather than EGCG was collected. Positive ESI-MS m/z with $(MH^+ - 18)$ at m/z 513 was detected. The combined fractions were concentrated and a portion of the residue was purified on RP-HPLC.

2.4 LC system

Prepacked silica gel (60 Å, 32–63 µm) columns (12 and 40 g) for normal phase chromatography were purchased from Teledyne Isco (Lincoln, NE, USA). Octadecyl (C_{18}) derivatized silica gel (60 Å) RP analytical and preparative columns for HPLC, purchased from YMC (Kyoto, Japan). Chiral analytical (4.6 mm × 250 mm) and preparative (20 mm × 250 mm) Chiralcel OD columns were purchased from Daicel Industries (Tokyo, Japan).

2.4.1 Flash column system

An automated flash chromatography system (Model Foxy 200, sg100, Teledyne Isco) equipped with a prepacked silica gel (particle size 35–60 µm) flash column from Teledyne Isco was used. The mobile phase for normal phase flash column consisted of ethyl acetate and hexanes in varying proportions, and the flow rate was varied between 40 and 60 mL/min depending on the column size. The eluent was monitored with a single channel UV detector at a wavelength of 254 nm.

2.4.2 HPLC system for RP purification of the crude adducts of EGCG and MGO

An automated HPLC from Gilson (Middleton, WI, USA) was used for preparative purpose. This semipreparative HPLC system was equipped with two pumps (322 HPLC pump with H2 pump heads), an UV-Vis DAD (155), and an automated injection system (215 liquid handler with syringe pump and 819 injection module). The mobile phase for the HPLC system was ACN and water (gradient method) with a flow rate set at 20 mL/min. The eluent was detected with dual UV wavelength at 326 and 254 nm.

2.4.3 HPLC system for chiral separation

An HPLC equipped with a pump (Waters Delta Prep 4000 delivery pump, Milford, MA, USA), UV-Vis detector (Waters 486 tunable absorbance detector), and an injector (Waters U6K injector) was used. A preparative (20 mm × 250 mm) Chiralcel OD column was used for the HPLC system. The mobile phase for the HPLC system was

40% absolute ethanol and 60% hexanes with a flow rate set at 5 mL/min. The eluent was detected with a UV wavelength at 326 nm.

2.5 NMR instrument

NMR spectra were recorded on a Varian 300 and Varian 500 Spectrometer (Varian, Palo Alto, CA, USA). With TMS serving as IS, 1H NMR was recorded at 300 and 500 MHz; ^{13}C NMR at 75 and 125 MHz.

2.6 LC-ESI-MS

An HPLC-MS system was composed of an auto-sampler injector (Switzerland), an HP1090 system controller with a variable UV wavelength (190–500 nm) detector, an evaporizing laser scattering deposition (ELSD) detector, and an ESI-MS detector from Micromass VG Platform II mass analyzer (Micromass, Beverly, MA, USA). ESI-MS conditions were as following: acquisition mode, ESI-positive; mass scan range, 100–800 amu; scan rate, 0.4 s; cone voltage, 25 V; source temperature, 150°C; probe temperature, 550°C. Analytical HPLC conditions on HPLC-MS: column, Chromabond WR C_{18} , 3 µm, 120 Å; length and OD, 30 mm × 3.2 mm; injection volume, 15 µL; flow rate, 2 mL/min; run time, 3 min. Mobile phase consisted of ACN and H_2O with 0.05% TFA, typical gradient of 10–90% ACN and the gradient varied.

2.7 Acetylation reaction

2.7.1 Acetylation of EGCG

EGCG (92 mg, 0.2 mmol) was suspended in a mixture of anhydrous methylene chloride (5 mL) and anhydrous pyridine (0.16 mL, 2 mmol), followed by dropwise addition of acetic anhydride (0.094 mL, 1 mmol). The resulted reaction mixture was stirred at 25°C for 12 h. Concentration of the reaction mixture and the resulted residue was dissolved in ethyl acetate (15 mL). The so formed organic solution was washed with water (× 2) and brine, dried over Na_2SO_4 , and concentrated. The residue was applied onto a silica gel flash column. The desired acetylated EGCG was eluted with ethyl acetate (40–100% in 12 min) and hexanes. Concentration of the collected fractions yielded 99 mg of the desired acetylated EGCG (Ac-EGCG) as a white solid. LC/MS for $C_{38}H_{34}O_{19}$ was 795 (MH^+), observed 817 (MNa^+). The NMR spectra were recorded on a Varian 300 Spectrometer (Varian), with trimethylsilane serving as IS for chemical shift reference.

2.7.2 Acetylation of EGCG + MGO adducts

Similar to the above reaction, after the LH-20 column, the residue containing the adduct of EGCG and MGO (25 mg,

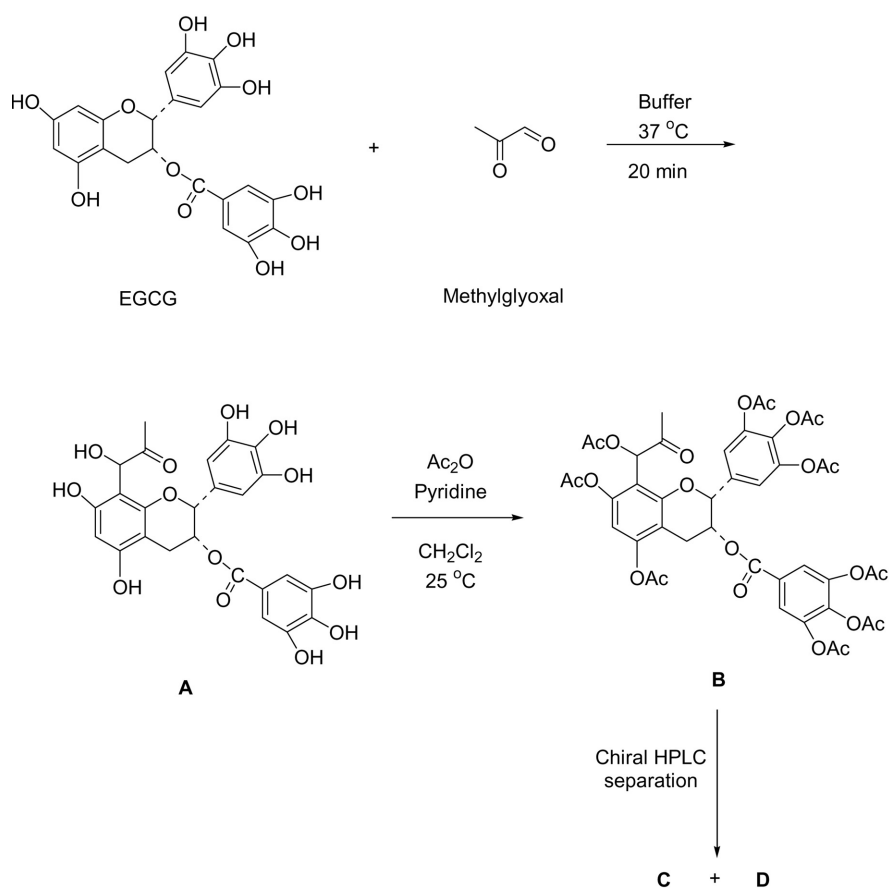


Figure 3. Formation of the adduct (A) of EGCG and methyl GO and its acetylation products (B, C, and D).

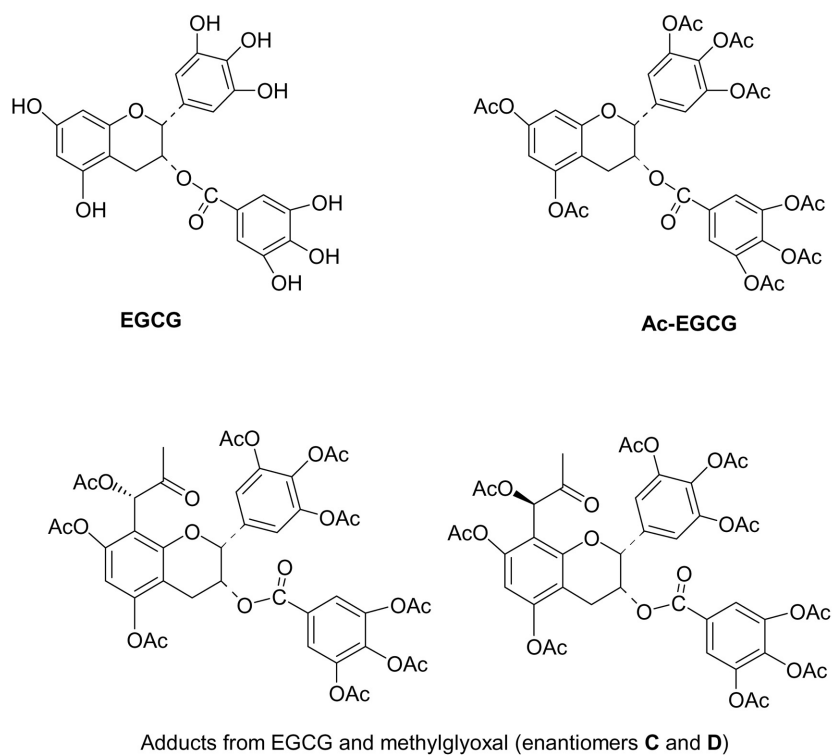


Figure 4. Structures of EGCG, acetylated EGCG (Ac-EGCG), and adducts C and D.

0.047 mmol) was suspended in a mixture of methylene chloride and pyridine (80 μ L, 1 mmol). Acetic anhydride (44 μ L, 0.47 mmol) was added dropwise, while the above mixture was cooled with ice bath. Upon the completion of addition, the cold bath was removed and the reaction mixture stirred at 25°C for 12 h. The mixture was concentrated at a reduced pressure and the residue was applied on silica gel flash column. Ethyl acetate and hexanes were the eluting solvents. The fractions that contained desired molecular weight by HPLC-ESI-MS were combined and concentrated. The desired product was yielded as a white solid (B, 9.1 mg). The formation of adduct A, its acetylation product B, and separation are shown in Fig. 3.

The white solid (B) was dissolved in a mixture of methylene chloride and ethanol (1:1). The solution was loaded onto an HPLC equipped with a chiral column. The eluting solvents were 60% hexanes and 40% ethanol. Two isolated products were obtained: 5.0 mg (C) and 2.5 mg (D). Their possible structures are shown in Fig. 4.

2.8 Optical rotation measurement

The optical rotation was measured (241 Polarimeter from Perkin-Elmer, sodium light) at 25°C in DMSO. $[\alpha]_D^{25}$ is -60° for C ($c = 3.7$ mg/mL) and -193° for D ($c = 2.3$ mg/mL).

2.9 NMR study of EGCG + MGO products

The structure elucidation of the products, C and D, from EGCG and MGO was based on NMR and MS analyses. As a reference, Ac-EGCG was analyzed in deuterated DMSO. Samples C (5 mg, retention time from chiral analytical HPLC, 12.5 min) and D (2.5 mg, retention time from chiral analytical HPLC, 10.2 min) were dissolved in deuterated DMSO, respectively. The NMR spectra were recorded on a Varian 500 Spectrometer (Varian), with tetramethylsilane serving as IS for chemical shift reference.

3 Results and discussion

3.1 Tea components trapping with RCS

MGO is a highly reactive alpha-dicarbonyl formed endogenously in numerous enzymatic and nonenzymatic reactions. MGO is very volatile and often coeluted with solvent peak when the mixture is prepared for GC analysis. Hence, many papers focused on environmental, clinical, or food studies had been published on its detection and quantification by the advantage of further chemical derivatization [11, 23–27]. After derivatization, it provides the specificity on analyte, which carries a unique functional group and is

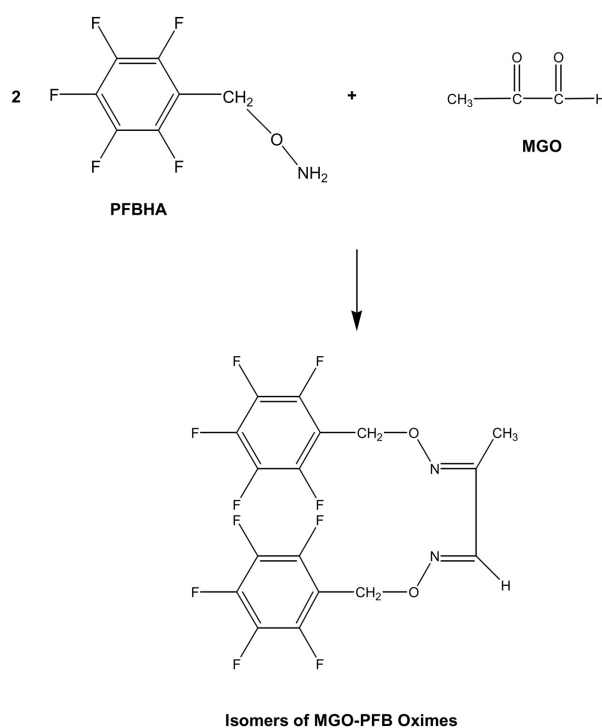


Figure 5. Reaction between PFBHA and MGO forming PFBHA–MGO oxims.

able to be detected with conventional detectors such as FID. In the present study, PFBHA was used as a carbonyl derivatization reagent. The chemical reaction between PFBHA and MGO is illustrated in Fig. 5. The *O*-PFB-oximes are the derivative compounds utilized in MGO quantification.

Figure 6 shows the chromatogram for derivatized MGO samples. There were six *O*-PFB-oximes peaks found after GC/FID analysis. Their retention times were at 35.19, 36.35, 38.18, 39.37, 39.78, and 40.18 min. In order to confirm their authentic identifications, the control sample was analyzed by GC/SIMMS (data are not shown). The mass spectra for the *O*-PFB-oximes are identical to those previously reported [27]. Thus, peaks 1 and 2 were the syn and anti-*O*-PFB-oxime stereoisomer derivatives of IS (2-chlorobenzaldehyde) and peaks 3, 4, 5, and 6 were the syn + syn, syn + anti, anti + syn, and anti + anti-*O*-PFB-oxime stereoisomer derivatives of MGO. The quantification of MGO-*O*-PFB-oxime compounds was based on the sum of these signals. The LOQ was determined as 5.1 μ g/L. The linear relationship between MGO concentrations used in this experiment and its *O*-PFB-oximes FID signals was confirmed.

The health beneficial effects of tea have been attributed mostly to their antioxidant and free radical scavenging properties. Their contributions to carbonyl stress have just been addressed in recent studies [20, 21]. The more detailed mechanism on the reaction has not been explored yet.

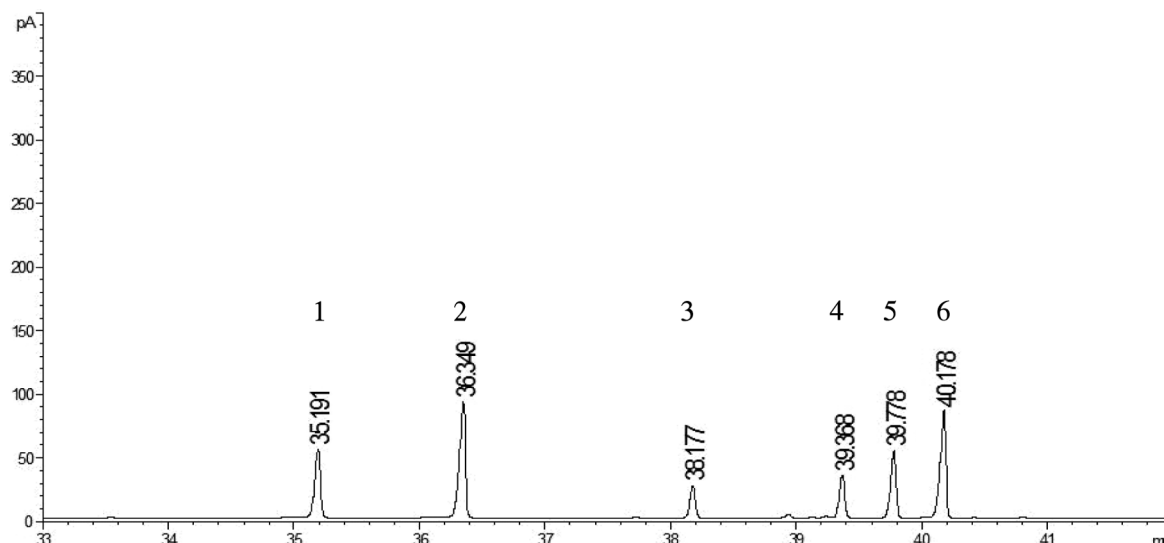


Figure 6. GC/FID chromatogram of MGO control sample (sample composition and treatment are shown in Fig. 1). Peaks 1 and 2 were due to syn- and anti-*o*-chlorobenzaldehyde (IS) *O*-PFB oximes. Peaks 3, 4, 5, and 6 were due to the syn + syn, syn + anti, anti + syn, and anti + anti MGO *O*-PFB oximes.

Hence, polyphenols in green and black tea are the key materials in this study. In the polyphenol adducts investigation, the molar ratio of MGO to each specific polyphenol was 3 and MGO decrease percentage (%) was compared with control sample at 0°C on ice/salt bath for 1 h. After 1 h at 37°C incubation, the MGO was very stable. Only 5.8% MGO decrease is shown in Fig. 7. Nevertheless, the partial catechin moiety of GA and PY were 17.1 and 27.8%, respectively. On one hand, among four catechins, the MGO decrease percentages were relatively close between ECG and PY. ECG showed the lowest decrease in catechins. On the other hand, EGC showed the highest decrease amount of MGO. From the result (45.7% decrease), which is more than one third, it is obvious that the active sites on EGC were more than one. Theaflavins, the main black tea component, was found to be more reactive with MGO. The decreased amounts of MGO in TF1, TF2, and TF3 were 63.1, 60.1, and 66.7%, respectively. The high levels of MGO reduction with respect to control samples indicated that theaflavins will be the excellent candidate for treatment of MGO scavenging in future *in vivo* studies. In addition, our results suggested that there were two MGO target sites on TF1, TF2, and TF3 when MGO completely reacted with theaflavin molecules under 1 h incubation time.

The next experiment was designed for the kinetic study of catechins and theaflavins. The $T_{1/2}$, the time for half of MGO remaining in a solution, was determined when the molar ratio of MGO to catechin or theaflavin was 1:1. For catechins as shown in Fig. 8, every catechin reacted promptly. EC had the highest reaction rate followed by ECG, EGC, and EGCG. $T_{1/2}$ equaled to 7.5 min for EGCG and less than 5 min for other catechins. In EC, 25% MGO

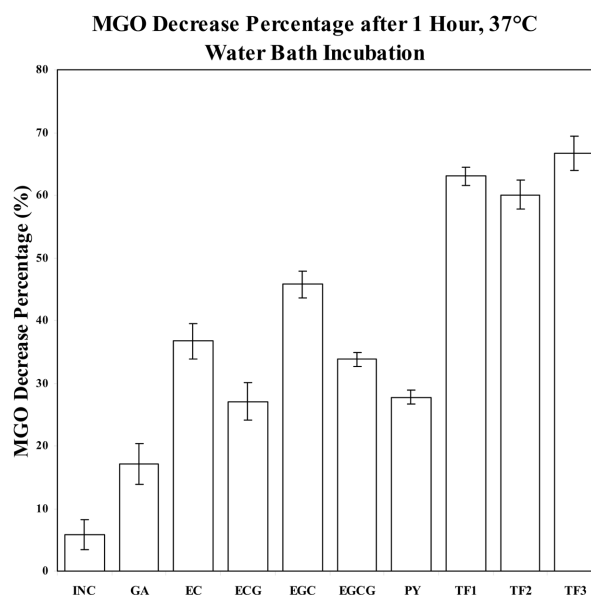


Figure 7. Comparison of the MGO decrease percentage among MGO only or added with each different polyphenol (37°C water bath, 40 rpm shaking speed); MGO control sample was kept in salt added ice bath. The decrease percentage values were expressed as mean \pm SD ($n = 3$). (INC: MGO only incubation sample).

remained after 5 min. The same reaction rate proceeded in ECG and EGC from 10 to 30 min. After 30 min, all catechins reached their maximum decrease values. EC reached 94%, ECG and EGC reached around 87–89%, and EGCG reached 77%. The shape of curves showed plateaus after 30 min in catechin samples. This indicated that reaction was completed after 30 min.

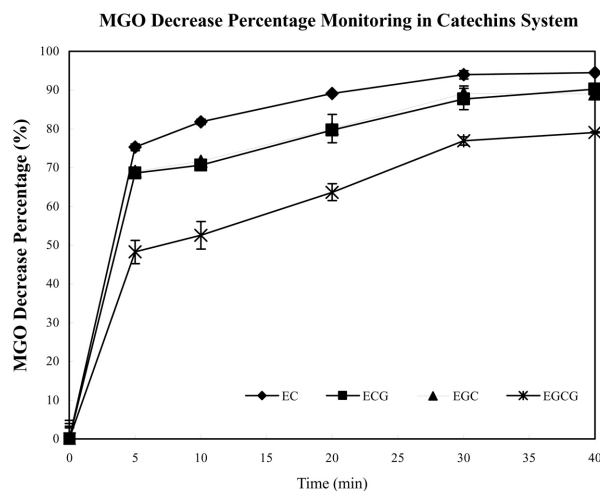


Figure 8. Kinetic study of green tea catechins and MGO in 1:1 molar ratio within 40 min time points at 37°C, and 40 rpm incubation speed. The values were expressed as mean \pm 1/2 range ($n = 2$). —●—: EC; —■—: ECG; —▲—: EGC; —×—: EGCG.

The similar pattern that appeared in theaflavin samples is shown in Fig. 9. $T_{1/2}$ equaled 4.7 min for TF1 and less than 4 min for TF2 and TF3. However, TF2 and TF3 reached plateaus after 20 min instead of 30 min in ECG and EGC. Only 6% further decreased after 20 min and finally the values reached 90% at 40 min. TF1 showed a gradual slope after 5 min and reached 77% decrease at 40 min.

3.2 MGO and EGCG adducts

The structures of EGCG, acetylated EGCG, and adducts C and D are shown in Fig. 4. The proton NMR of the acetylated EGCG in DMSO- d_6 was as expected; the six aromatic protons of acetylated EGCG are clearly seen. The singlet peak at 7.53 ppm is the two identical aromatic protons of gallate. The other singlet at 7.38 ppm represents the two identical aromatic protons at B-ring of EGCG. The protons of H₆ (6.77 ppm, 1H, doublet) and H₈ (6.64 ppm, 1H, doublet) are not equivalent with a coupling constant of 2.4 Hz, following a typical meta–meta coupling range, which showed a dramatic environmental change for these two protons after the acylation. A broad peak at 5.60 ppm indicates that the H₃ proton is due to multiple couplings with two nonequivalent H₄ protons and a chiral H₂ proton. The H₂ proton showed a broad peak at 5.26 ppm, because of the weak couplings between the equatorial proton H₂ and axial proton H₃. The doublet of doublet peak at 3.14 ppm is the axial proton of H₄ which has couplings with an equatorial proton of H₄ ($J = 17.4$ Hz) and an axial proton of H₃ ($J = 3.6$ Hz). The equatorial proton of H₄ shows a doublet at 2.95 ppm with a coupling constant of 17.4 Hz. The eight methyl groups appeared in the range of 2.22–2.23 ppm. The

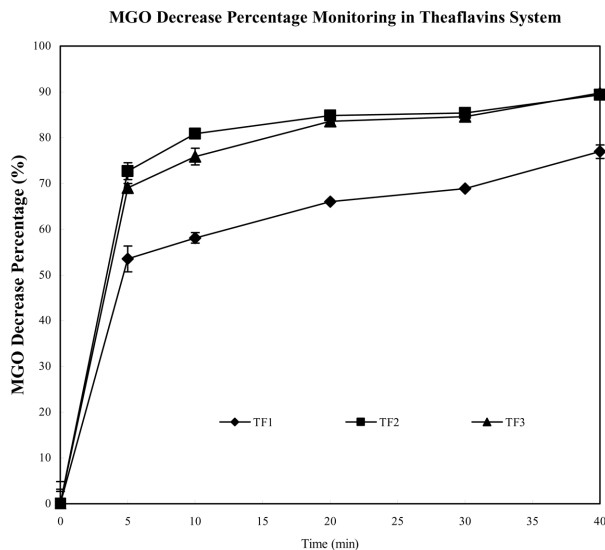
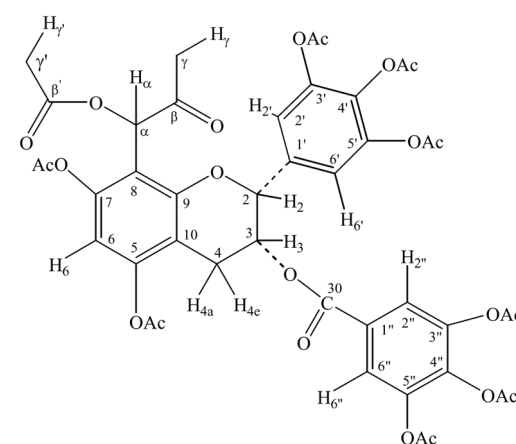


Figure 9. The kinetic study of black tea theaflavins and MGO in 1:1 molar ratio within 40 min time points at 37°C, 40 rpm incubation speed. Duplicate samples were performed at every time point. The values were expressed as mean \pm 1/2 range. —●—: TF1; —■—: TF2; —▲—: TF3.

carbon-13 NMR (DMSO- d_6) showed the nine carbonyl carbons of EGCG at 169.89, 169.49, 168.87, 168.87, 168.80, 168.80, 168.06, 167.72, and 164.27 ppm and 18 aromatic carbon atoms at 155.57, 150.77, 150.51, 144.45, 144.15, 140.01, 136.76, 135.38, 128.13, 123.00, 122.54, 120.34, 119.89, 111.07, 110.52, 110.19, 109.10, and 108.75 ppm. The carbon atoms on the eight methyl groups are found at 22.05, 21.75, 21.60, 21.47, 21.29, 21.16, 21.05, and 20.74 ppm.

The proton NMR of the purified adduct A from EGCG and MGO was obtained and it showed a minimum of two adducts existing in A. Efforts had been embarked to purify the adduct A using silica gel chromatography, RP-HPLC, and supercritical fluid chromatography (SFC), but failed due to the instability of the adduct A at the normally performed conditions such as ambient temperature, judged by polymer-like proton NMRs. Therefore, further acetylation of the adduct A was designed to stabilize the adduct A formed from EGCG and MGO. Similar to the acetylation reaction of EGCG, the adduct A was acylated with acetic anhydride under the presence of pyridine in an anhydrous media, to yield the acetylated adduct B by HPLC-ESI-MS ($MNa^+ = 931$). After purification from silica gel chromatography and RP-HPLC, the NMR of adduct B still showed a mixture of compounds. Therefore, separation efforts had been focused on possible mixtures of regioisomers between 6- and 8-substitution and newly generated stereoisomers. Using chiral HPLC technology, the adduct B was eventually separated into two enantiomers, adducts C and D, by a chiral separation technique. From the MS data of 931

Table 1. ^1H NMR data (ppm) of acetylated EGCG and adducts C and D in $\text{DMSO}-d_6$


	H_2	H_3	H_{4e}	H_{4a}	H_6	H_8
Ac-EGCG	5.26 (br, 1H)	5.60 (br, 1H)	2.95 (d, $J = 17.4$ Hz, 1H)	3.14 (dd, $J = 17.4$ and 3.6 Hz, 1H)	6.77 (d, $J = 2.4$ Hz, 1H)	6.64 (d, $J = 2.4$ Hz, 1H)
Adduct C	5.62 (s, 1H)	5.69 (br, 1H)	3.02 (d, $J = 17.4$ Hz, 1H)	3.17 (dd, $J = 17.4$ and 3.6 Hz, 1H)	6.77 (s, 1H)	
Adduct D	5.65 (s, 1H)	5.63 (br, 1H)	3.01 (d, $J = 17.4$ Hz, 1H)	3.18 (dd, $J = 17.4$ and 3.6 Hz, 1H)	6.77 (s, 1H)	
	$\text{H}_{2'}, \text{H}_{6'}$	$\text{H}_{2''}, \text{H}_{6''}$	H_α	H_γ	$\text{H}_{\gamma'}$	$\text{H}-\text{CH}_2\text{CO}-$
Ac-EGCG	7.38 (s, 2H)	7.53 (s, 2H)				2.22–2.23 (24H)
Adduct C	7.40 (s, 2H)	7.47 (s, 2H)	6.44 (s, 1H)	2.08 (s, 3H)	2.10 (s, 1H)	2.26–2.31 (24H)
Adduct D	7.32 (s, 2H)	7.54 (s, 2H)	6.49 (s, 1H)	2.15 (s, 3H)	2.07 (s, 3H)	2.31–2.65 (24H)

(MNa^+), we could deduce that the adduct B, C, or D was formed from one mol of EGCG and one mole of MGO in PBS solution after 20 min incubation.

The proton and C^{13} NMR spectral data of adduct C and D are listed in Tables 1 and 2. Both proton NMR and carbon NMR showed the existence of nine acetyl groups. The chemical shift at 200.90 ppm is a diagnostic resonance for a ketone carbonyl carbon, indicating the presence of a ketone functional group. By comparing the proton NMR of adduct C with that of acetylated EGCG, we could assign the following protons with the assistance of heteronuclear single-quantum correlation (HSQC) 2-D NMR: H_2 at 5.62 ppm, H_3 at 5.69 ppm, two protons of H_4 at 3.02 and 3.17 ppm, respectively, H_6 at 6.77 ppm (singlet), $\text{H}_{2'}$ and $\text{H}_{6'}$ at 7.40 ppm, and the protons on the pyrogallate ring at 7.47 ppm. Comparing the doublet resonance of proton H_6 on the acetylated EGCG, the singlet nature of H_6 in adduct C hints the absence of H_8 , whose chemical shift is around 6.64 ppm, indicating the loss of the proton at this position. Due to the lack of conjugation, the newly formed carbon–carbon single bond ($\text{C}_8-\text{C}_\alpha$) has none or minor impact on the resonance of H_6 . The chemical environment of H_6 has little change. Therefore, by comparing the resonance of H_6

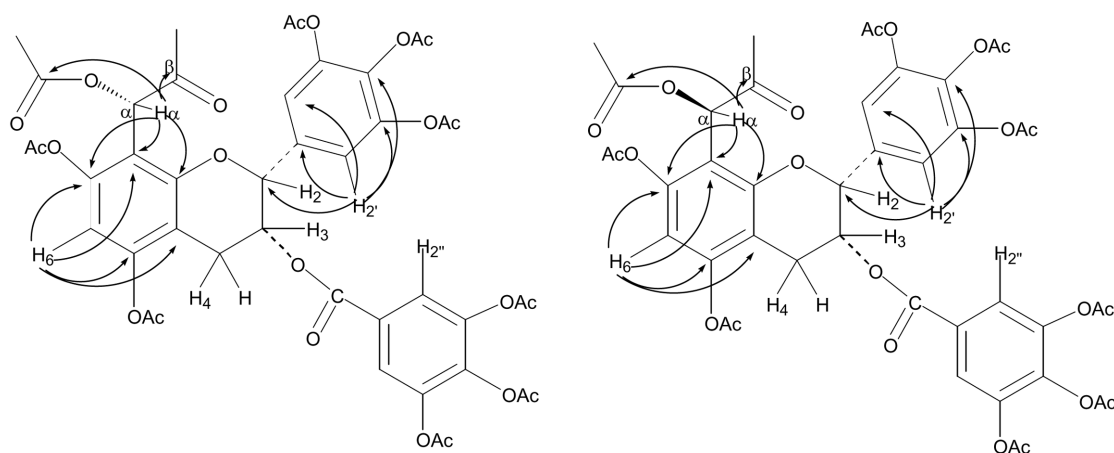
in C and D with that of acetylated EGCG, we can deduce that H_6 is unattacked, meaning the reaction occurred at position 8 of EGCG. There is a newly appeared proton (H_α) at 6.44 ppm. Its singlet resonance shows no correlation with proton H_6 and it is connected with a nonaromatic carbon from HSQC (70.84 ppm), indicating it is the original aldehyde proton of MGO. Also, from HSQC experiment, the following resonances can be assigned: C_6 at 110.10 ppm, C_α at 70.45 ppm, C_2 at 76.33 ppm, C_3 at 67.77 ppm, C_4 at 25.27 ppm, and some carbons on the B-ring and gallate.

In the heteronuclear multiple quantum multiple bond correlation (HMBC) experiment, the correlations between H_α ($\delta_{\text{H}} = 6.44$ ppm) and C_β ($\delta_{\text{C}} = 200.90$ ppm), C_7 ($\delta_{\text{C}} = 25.54$ ppm), C_8 ($\delta_{\text{C}} = 113.07$ ppm), C_7 ($\delta_{\text{C}} = 148.20$ ppm), and C_9 ($\delta_{\text{C}} = 152.35$ ppm) established the connection of $\text{C}_7-\text{C}_8-\text{C}_\alpha-\text{C}_\beta-\text{C}_7\text{H}_3$, *i.e.*, the connection between C_8 and the original aldehyde carbon of MGO ($\text{O}=\text{C}_\alpha\text{H}-\text{C}_\beta(\text{O})-\text{C}_7\text{H}_3$). This connection also explains the singlet of H_α ($\delta_{\text{H}} = 6.44$ ppm) and H_6 ($\delta_{\text{H}} = 6.77$ ppm). More evidences come from the correlations between H_6 ($\delta_{\text{H}} = 6.77$ ppm) and C_7 ($\delta_{\text{C}} = 148.20$ ppm), C_5 ($\delta_{\text{C}} = 149.75$ ppm), C_{10} ($\delta_{\text{C}} = 110.36$ ppm) and C_8 ($\delta_{\text{C}} = 113.07$ ppm). The two protons on the B-ring of EGCG were untouched judged from

Table 2. ^{13}C NMR data (ppm) of acetylated adducts C and D in $\text{DMSO}-d_6$

	C_2	C_3	C_4	C_5	C_6	C_7	C_8	C_9	C_{10}
C	75.95	67.86	25.11	149.75	110.21	148.20	113.07	152.35	110.36
D	76.33	67.77	25.27	149.84	110.10	148.06	113.70	152.70	110.24
	$\text{C}_{1'}$	$\text{C}_{2'}$	$\text{C}_{3'}$	$\text{C}_{4'}$	$\text{C}_{5'}$	$\text{C}_{6'}$			
C	133.70	118.35	135.25	142.82	135.25	118.35			
D	133.90	118.63	135.44	142.85	135.44	118.63			
	$\text{C}_{1''}$	$\text{C}_{2''}$	$\text{C}_{3''}$	$\text{C}_{4''}$	$\text{C}_{5''}$	$\text{C}_{6''}$			
C	126.74	121.44	138.76	143.05	138.76	121.44			
D	126.64	121.72	138.82	143.14	138.82	121.72			
	C_α	C_β	C_γ	$\text{C}_{\beta'}$	$\text{C}_{\gamma'}$	C_{30}			
C	70.84	200.90	25.54	168.99	19.86	162.58			
D	70.45	202.59	26.08	169.40	20.12	162.56			

In compound C: ^{13}C for $-\text{CH}_3$ in acetyl groups are in 20.03–20.24 ppm. ^{13}C for acetyl carbonyl are in 166.66–168.65 ppm. In compound D: ^{13}C for $-\text{CH}_3$ in acetyl group are in 19.82–20.52 ppm. ^{13}C for acetyl carbonyl are in 166.73–168.63 ppm.

**Figure 10.** HMBC correlations of adducts C and D.

their proton integration and the correlations between H_2 ($\delta_{\text{H}} = 7.40$ ppm) and $\text{C}_{1'}$ ($\delta_{\text{C}} = 133.70$ ppm), C_2 ($\delta_{\text{C}} = 75.95$ ppm), $\text{C}_{3'}$ ($\delta_{\text{C}} = 135.25$ ppm), $\text{C}_{6'}$ ($\delta_{\text{C}} = 118.33$ ppm), and $\text{C}_{4'}$ ($\delta_{\text{C}} = 142.82$ ppm). The same analogy applies to the untouched protons on the pyrogallate aromatic ring. Figure 10 demonstrates the HMBC correlations of adduct C.

Further confirmation of the connection between C_8 and C_α (the original aldehyde carbon of MGO) came from rotating frame nuclear overhauser effect spectroscopy (ROESY) 2-D NMR experiment. The detection of through-space interaction between H_α ($\delta_{\text{H}} = 6.44$ ppm) and $\text{H}_{2'}$ and $\text{H}_{6'}$ ($\delta_{\text{H}} = 7.40$ ppm) evidenced the connection between C_8 of EGCG and C_α (aldehyde carbon of MGO). The existence of the through space coupling between $\text{H}_{2'}$ or $\text{H}_{6'}$ and H_α in the adducts of MGO and EGCG, has the support from molecular modeling calculation which shows the shortest distance between $\text{H}_{2'}$ or $\text{H}_{6'}$ and H_α being 2.91 Å for “*R*”-isomer and 3.31 Å for “*S*”-isomer in the minimized structures (Soft-

ware: Forcefield MMFF94X, MOE 2005). Whereas with the same molecular modeling tool, if the connection was between C_6 and the aldehyde carbon of MGO, the measured distance between $\text{H}_{2'}$ or $\text{H}_{6'}$ and H_α (original aldehyde proton of MGO) being 7.29 Å for *R*-isomer and 8.54 Å for *S*-isomer in the minimized structure, impossible to observe NOE in the NMR experiments. The space correlations are illustrated in Fig. 11.

The NMR data of adduct D are also listed in Tables 1 and 2. Same 2-D NMR (HSQC, HMBC, and ROESY) analysis of adduct D revealed that it is an enantiomer of adduct C, existing with exact by the same correlations between H_α ($\delta_{\text{H}} = 6.49$ ppm) and C_8 ($\delta_{\text{C}} = 113.70$ ppm), C_7 ($\delta_{\text{C}} = 148.06$ ppm), C_9 ($\delta_{\text{C}} = 152.70$ ppm), C_β ($\delta_{\text{C}} = 202.36$ ppm); H_6 ($\delta_{\text{H}} = 6.77$ ppm) and C_7 , C_5 ($\delta_{\text{C}} = 149.84$ ppm), C_{10} ($\delta_{\text{C}} = 110.24$ ppm) in HMBC. Again, evidence from ROESY experiment showed the through space coupling between H_α ($\delta_{\text{H}} = 6.49$ ppm) and $\text{H}_{2'}$ or $\text{H}_{6'}$ ($\delta_{\text{H}} = 7.32$ ppm).

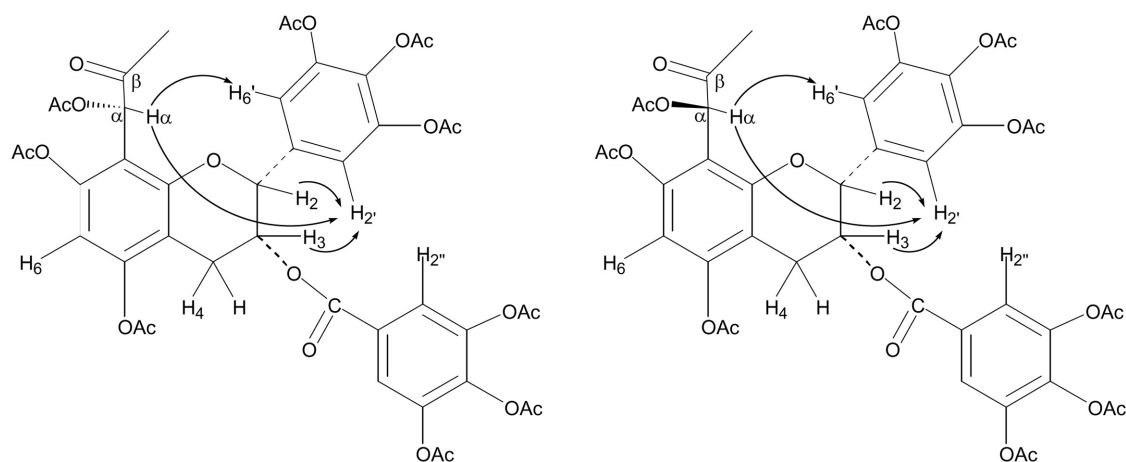


Figure 11. ROSEY correlations of adducts C and D.

The HMBC and ROSEY correlations are structurally illustrated in Figs. 10 and 11.

From the MS results and the NMR analyses of the adducts formed from the reaction between EGCG and MGO, we can conclude that the reaction dominantly occurs at the 8-position of EGCG. The nuclear attack of electron deficient aldehyde carbonyl carbon by electron rich nucleophile, specifically C₈ position of EGCG, formed the EGCG-MGO adducts as enantiomers. Other adducts, such as the products formed between C₆ position of EGCG and MGO, were not observed and isolated in this study. The determination of absolute configuration of adducts C and D is in progress. Furthermore, this adduct evidence may apply to theaflavin compounds which are the further oxidation product of catechins. The two reactive sites could be on the eight positions of the original catechins before the formation of conjugated benzotropolone structure.

4 Concluding Remarks

Our observation of the direct and rapid reaction of tea polyphenols with MGO may provide a new mechanism by which polyphenol-rich foods and beverages can have a positive effect on human health.

5 References

- [1] Abele, D., *Nature* 2002, 420, 27.
- [2] Lunec, J., *J. Int. Fed. Clin. Chem.* 1992, 4, 58, 60–63.
- [3] Thornalley, P. J., Battah, S., Ahmed, N., Karachalias, N. *et al.*, *Biochem. J.* 2003, 375, 581–592.
- [4] Fu, M. X., Wells-Knecht, K. J., Blackledge, J. A., Lyons, T. J. *et al.*, *Diabetes* 1994, 43, 676–83.
- [5] Shimoi, K., Okitsu, A., Green, M. H. L., Lowe, J. E. *et al.*, *Mutat. Res.* 2001, 480–481, 371–378.
- [6] Miyata, T., Sugiyama, S., Saito, A., Kurokawa, K., *Kidney Int. Suppl.* 2001, 78, S25–S31.
- [7] Baynes, J. W., *Clin. Chem. Lab. Med.* 2003, 41, 1159–1165.
- [8] Bonnefont-Rousselot, D., *Curr. Opin. Clin. Nutr. Metab. Care* 2002, 5, 561–568.
- [9] Knight, J. A., *Ann. Clin. Lab. Sci.* 1995, 25, 111–121.
- [10] Hodge, J. E., *J. Agric. Food Chem.* 1953, 1, 928–943.
- [11] Hayashi, T., Shibamoto, T., *J. Agric. Food Chem.* 1985, 33, 1090–1093.
- [12] De Revel, G., Pripis-Nicolau, L., Barbe, J.-C., Bertrand, A., *J. Sci. Food Agric.* 2000, 80, 102–108.
- [13] Reichard, G. A., Skutches, C. L., Hoeldtke, R. D., Owen, O. E., *Diabetes* 1986, 35, 668–674.
- [14] Lyles, G. A., Chalmers, J., *Biochem. Pharmacol.* 1992, 43, 1409–1414.
- [15] Phillips, S. A., Thornalley, P. J., *Eur. J. Biochem.* 1993, 212, 101–105.
- [16] Thornalley, P. J., Langborg, A., Minhas, H. S., *Biochem. J.* 1999, 344, 109–116.
- [17] Frischmann, M., Bidmon, C., Angerer, J., Pischetsrieder, M., *Chem. Res. Toxicol.* 2005, 18, 1586–1592.
- [18] Thornalley, P. J., *Chem. Biol. Interact.* 1998, 111–112, 137–151.
- [19] Rahbar, S., Yerneni, K. K., Scott, S., Gonzales, N. *et al.*, *Mol. Cell Biol. Res. Commun.* 2000, 3, 360–366.
- [20] Wu, C.-H., Yen, G.-C., *J. Agric. Food Chem.* 2005, 53, 3167–3173.
- [21] Peterson, D. G., Totlani, V. M., *J. Agric. Food Chem.* 2005, 53, 4130–4135.
- [22] Huang, M.-T., Liu, Y., Ramji, D., Lo, C.-Y. *et al.*, *Mol. Nutr. Food Res.* 2006, 50, 115–122.
- [23] De Revel, G., Bertrand, A., *J. Sci. Food Agric.* 1993, 61, 267–272.
- [24] Martineau, B., Acree, T. E., Henick-Kling, T., *Food Res. Int.* 1995, 28, 139–143.
- [25] Akira, K., Matsumoto, Y., Hashimoto, T., *Clin. Chem. Lab Med.* 2004, 42, 147–153.
- [26] Glomb, M., Tschirnich, R., *J. Agric. Food Chem.* 2001, 49, 5543–5550.
- [27] Lapolla, A., Flamini, R., Vedova, A. D., Senesi, A. *et al.*, *Clin. Chem. Lab Med.* 2003, 41, 1166–1173.